The filament (shown in Fig. 3A as a linear structure for simplicity) is more likely to be compacted in a solenoid in which the DNA wraps through multiple turns about a protein core, as was suggested by the observed changes in linking numbers upon formation of a SopB-DNA complex (*19*).

Prokaryotic centromeres are characterized by the presence of arrays of sites to which one of the partition proteins bind. There are 6 sites in P1 (Fig. 1A), 12 in F, 10 in R1, and 12 in pTAR (*20*). Whereas these plasmid-borne binding sites are tightly clustered, the several chromosomal binding sites for the *Bacillus subtilis* partition (and sporulation) protein Spo0J are distributed over a region spanning many kilobases (*3*). The centromere may serve as a handle that is used to tether or orient a large structure, with its several binding sites facilitating a steady grip or the formation of an intermediate that is appropriately paired for partitioning. Evidence for paired intermediates in the partitioning of plasmid R1 and involving its cognate ParB analog has recently been obtained (*21*). Like the proteins of heterochromatin that spread from centromeres or telomeres of eukaryotic chromosomes, the ParB that spreads from the P1 plasmid centromere can silence genes. In each case, this capacity for gene silencing may be incidental to a primary structural role that is associated with DNA segregation or movement.

References and Notes

1. E. A. Russo, R. A. Martienssen, A. D. Riggs, Eds., *Epigenetic Mechanisms in Gene Regulation* (Cold Spring Harbor Laboratory Press, Plainview, NY, 1996).
2. R. C. Allshire, E. R. Nimmo, K. Ekwall, J. P. Javerzat, G. Cranston, *Genes Dev.* **9**, 218 (1995); G. H. Karpen, *Curr. Opin. Genet. Dev.* **4**, 281 (1994).
3. D. C.-H. Lin, P. A. Levin, A. D. Grossman, *Proc. Natl. Acad. Sci. U.S.A.* **94**, 4721 (1997).
4. D. A. Mohl and J. W. Grober, *Cell* **88**, 675 (1998); C. D. Webb *et al.*, *ibid.*, p. 667.
5. D. C.-H. Lin and A. D. Grossman, *ibid.* **92**, 675 (1998).
6. A. S. Lynch and J. C. Wang, *Proc. Natl. Acad. Sci. U.S.A.* **92**, 1896 (1995); S.-K. Kim and J. C. Wang, *ibid.* **95**, 1523 (1998).
7. R. Hanai *et al.*, *J. Biol. Chem.* **271**, 17469 (1996).
8. A. L. Abeles, S. A. Friedman, S. J. Austin, *J. Mol. Biol.* **185**, 261 (1985); published errata, *ibid.* **189**, 387 (1986).
9. B. E. Funnell, *J. Biol. Chem.* **266**, 14328 (1991).
10. _____ and L. Gagnier, *ibid.* **268**, 3616 (1993); F. Hayes and S. J. Austin, *Proc. Natl. Acad. Sci. U.S.A.* **90**, 9228 (1993).
11. M. A. Davis, K. A. Martin, S. J. Austin, *Mol. Microbiol.* **6**, 1141 (1992).
12. M. Łobocka and M. Yarmolinsky, *J. Mol. Biol.* **259**, 366 (1996).
13. The *parS*-bearing plasmid pMLO6 (*12*) could not be maintained in the presence of a source of ParB. By moving *parS* ~180° from its position in pMLO6, a plasmid was created that, in the presence of ParB, no longer conferred spectinomycin resistance but had become only moderately unstable. The altered distance of *parS* from the DNA loci that are involved in replication and in the expression of antibiotic resistance can account for the difference in phenotypes.
14. B. E. Funnell, *Proc. Natl. Acad. Sci. U.S.A.* **85**, 6657 (1988).
15. O. Rodionov and M. Yarmolinsky, data not shown.
16. K. A. Martin, M. A. Davis, S. J. Austin, *J. Bacteriol.* **173**, 3630 (1991); M. Łobocka and M. Yarmolinsky, unpublished material.
17. B. E. Funnell and L. Gagnier, *Biochimie* **76**, 924 (1994).
18. K. Gerdes, unpublished material.
19. D. P. Biek and J. Shi, *Proc. Natl. Acad. Sci. U.S.A.* **91**, 8027 (1994); A. S. Lynch and J. C. Wang, *J. Mol. Biol.* **236**, 679 (1994).
20. M. Helsberg and R. Eichenlaub, *J. Bacteriol.* **165**, 1043 (1986); M. Dam and K. Gerdes, *J. Mol. Biol.* **236**, 1289 (1994); D. R. Gallie and C. L. Kado, *ibid.* **193**, 465 (1987).
21. R. B. Jensen, R. Lurz, K. Gerdes, *Proc. Natl. Acad. Sci. U.S.A.* **95**, 8550 (1998).
22. K. F. Wertman, A. R. Wyman, D. Botstein, *Gene* **49**, 253 (1986).
23. L. Diederich, L. J. Rasmussen, W. Messer, *Plasmid* **28**, 14 (1992).
24. P. P. Papp, G. Mukhopadhyay, D. K. Chattoraj, *J. Biol. Chem.* **269**, 23563 (1994).
25. T. Som and J.-I. Tomizawa, *Mol. Gen. Genet.* **187**, 375 (1982).
26. V. M. Morales, A. Baeckman, M. Bagdasarian, *Gene* **97**, 39 (1991).
27. J. H. Miller, *Experiments in Molecular Genetics* (Cold Spring Harbor Laboratory Press, Plainview, NY, 1972); W. V. Shaw, in *Antibiotics*, vol. 43 of *Methods in Enzymology*, J. H. Hash, Ed. (Academic Press, New York, 1975), pp. 737–755; E. Brickman and J. Beckwith, *J. Mol. Biol.* **96**, 307 (1975).
28. Constructs 0, I, and II were derived from a *recA56* MC1061 (*22*) by the integration of *parS*, *lacZ*, and *cat* into *att*λ (*23*). The *lacZ* gene under control of the P1 *repA* promoter (P_{repA}), accompanied upstream by four *rrnB* T1 transcription terminators, was from pPP112 (*24*). The source of *parS* was a 298–base pair Eco RI fragment from pBEF143 (*9*). The *cat* gene was from pST52 (*25*). A mutant version of construct I that is constitutive for *phoA* expression was used for the alkaline phosphatase assay. Gene orientations and the absence of duplicate insertions were determined by restriction mapping.
29. To construct pOAR32, we cloned the *parB* gene under tac promoter (P_{tac}) control in a derivative of pMMB67EH (*26*) in which the kanamycin-resistance gene of transposon (Tn) *903* had been inserted so as to disrupt the *bla* gene of the vector. For assays, cultures were grown in LB broth (*27*) with kanamycin (25 mg/ml) and, subsequently, for about six generations, with isopropyl-β-D-thiogalactopyranoside (IPTG) at several concentrations before the measurement of enzyme specific activities. The ParB concentration in sonicated cell extracts was estimated by the ECL protein immunoblotting analysis system (Amersham) with highly purified ParB as standard.
30. T. Takano and S. Ikeda, *Virology* **70**, 198 (1976).
31. B. P. Nichols and C. Yanofsky, in *Recombinant DNA, Part C*, vol. 101 of *Methods in Enzymology*, R. Wu, L. Grossman, K. Moldave, Eds. (Academic Press, New York, 1983), pp. 155–164.
32. Template DNAs were purified with a high pure PCR template preparation kit (Boehringer Mannheim) and, unless otherwise indicated, used at a dilution of 1:850. PCR reactions were performed with 100 pmoles of each primer and 0.25 units of Taq polymerase in B buffer (Promega) in 50-μl volumes as follows: An initial denaturation at 95°C for 2 min was followed by 25 cycles with denaturation for 30 s at 95°C, annealing for 30 s at 61°C (at 54°C with primers directed against P1 DNA), polymerization for 1 min at 72°C, and a final 2-min extension at 72°C.
33. Single-letter abbreviations for the amino acid residues are as follows: D, Asp; E, Glu; G, Gly; I, Ile; K, Lys; L, Leu; P, Pro; Q, Gln; R, Arg; T, Thr; and V. Val.
34. A. L. Abeles, K. M. Snyder, D. K. Chattoraj, *J. Mol. Biol.* **173**, 307 (1984).
35. D. K. Chattoraj, K. Cordes, A. L. Abeles, *Proc. Natl. Acad. Sci. U.S.A.* **81**, 6456 (1984).
36. M. Łobocka, M. Rusin, A. Samojedny, unpublished material.

37. We thank D. K. Chattoraj for valuable discussions, bacterial strains, plasmids, and antibody to RepA, and, with R. A. Weisberg, for critical readings of early versions of the manuscript; K. Gerdes for permission to cite unpublished material; B. E. Funnell for a sample of highly purified ParB; and D. C.-H. Lin for the cross-linking immunoprecipation protocol that he developed in the A. D. Grossman laboratory. O.R. and M.L. were supported by Fogarty postdoctoral fellowships.

17 August 1998; accepted 22 December 1998

The Role of Locus Coeruleus in the Regulation of Cognitive Performance

Marius Usher, Jonathan D. Cohen, David Servan-Schreiber, Janusz Rajkowski, Gary Aston-Jones*

Noradrenergic locus coeruleus (LC) neurons were recorded in monkeys performing a visual discrimination task, and a computational model was developed addressing the role of the LC brain system in cognitive performance. Changes in spontaneous and stimulus-induced patterns of LC activity correlated closely with fluctuations in behavioral performance. The model explains these fluctuations in terms of changes in electrotonic coupling among LC neurons and predicts improved performance during epochs of high coupling and synchronized LC firing. Cross correlations of simultaneously recorded LC neurons confirmed this prediction, indicating that electrotonic coupling in LC may play an important role in attentional modulation and the regulation of goal-directed versus exploratory behaviors.

Neuromodulators, such as norepinephrine (NE) and dopamine, have long been thought to play a role in regulating nonspecific aspects of behavior, such as motivation and arousal. However, recent evidence indicates that these systems may play a more specific role in task-related cognitive processes. Brainstem dopaminergic neurons respond selectively to stimuli that predict reward (*1*). Stimulus-specific activity has also been observed in LC neurons. Recent studies found that LC neurons in monkeys performing a visual discrim-

ination task exhibited short-latency stimulus-evoked (phasic) responses to target (CS+) stimuli but not to distractor (CS−) stimuli or other task events (*2*). The latencies of these LC responses were substantially shorter than, and temporally correlated with, the latencies of corresponding behavioral responses, indicating that LC activity may affect task responding. However, the mechanisms that govern LC activity or its effect on behavior have remained unclear.

LC neurons were recorded in four Cynomolgus monkeys performing a visual discrimination task (*2*). This task required the monkey to respond to infrequent visual target stimuli but not to frequent distractors (*3*). In many of our recordings, LC neurons changed levels of tonic discharge several times (Fig. 1A), in association with alterations in task performance. We divided behavioral performance into epochs of "good" and "poor" performance, on the basis of the frequency of false alarm (FA) errors produced [as described previously (*2*, *4*)]. Signal detection sensitivity (d') was substantially higher in epochs of good compared with those of poor performance, so the difference between these cannot be explained by a simple change in response criterion (*4*). Furthermore, although mean lever response times (RTs) were not systematically different between the two levels of performance, there was a significant narrowing of the distribution of lever release latencies during the good epochs (*4*) (Fig. 1B).

As shown in Fig. 1A, epochs of poor performance were associated with significantly higher tonic LC activity than were epochs of good performance (3.0 ± 0.3 spikes/s compared with 2.0 ± 0.2 spikes per second $P < 0.001$; FA frequencies were 7.6 ± 0.9% compared with 1.0 ± 0.2% of trials; $P < 0.01$; $n = 30$ cells; paired t tests). Similar results were obtained in an additional 37 multicell LC recordings. Thus, in addition to our previous finding of a close relation between phasic LC discharge and behavioral responses (*2*), we also found a close relation between the level of LC tonic activity and behavioral performance. We refer to the lower level of tonic LC activity during epochs of good performance as "intermediate," to distinguish it from the low (near zero) level typically associated with drowsiness or sleep (*2*, *5*).

We also found that sensory-evoked LC responses varied with the level of tonic LC activity and task performance. The phasic responses that LC neurons exhibit selectively for target stimuli in this task occurred almost exclusively during epochs of intermediate tonic LC activity and good task performance (Fig. 1, C to F). For the 30 single-cell recordings described above, response magnitudes to target stimuli during epochs of good performance were significantly greater than during epochs of poor performance (2.7 ± 0.4 compared with 0.8 ± 0.2; $P < 0.001$; paired t test). Thus, increased tonic LC discharge was associated with decreased responsivity of LC neurons to target stimuli as well as decreased task performance. This three-way association of tonic LC activity, LC phasic responses to target stimuli, and level of task performance was observed consistently across our recordings.

These results suggest that there is a precise relation between LC activity and behavioral performance. To elucidate the mechanisms that might underlie this relation, we developed a computational model of LC function and its effect on performance in this task.

The model is a hybrid, with two primary components: an LC network and a stimulus discrimination (behavioral) network (Fig. 2A). The LC network is relatively fine-grained and designed to simulate physiological mechanisms underlying LC function, whereas the behavioral network is the simplest capable of simulating performance in the visual discrimination task. Although the use of such a hybrid model that combines components at different levels of abstraction may be unusual, this is justified by the correspondence between each component of the model and the

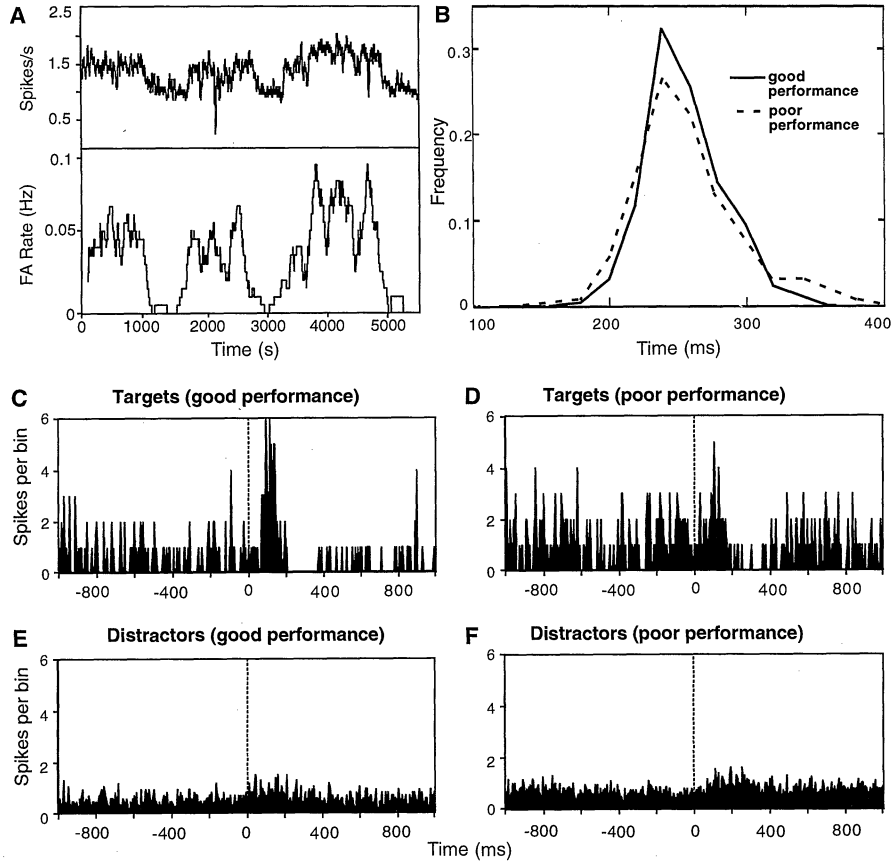

Fig. 1. Representative data from a typical LC neuron recorded in a monkey during performance of the visual discrimination task. (**A**) The rate of discharge for an LC cell (top curve) and the number of FAs (bottom curve), both integrated for a sliding window of 20 s. (**B**) Normalized distributions for behavioral response latencies (lever releases) during "good" epochs (solid line) compared with "poor" epochs (dashed line) averaged for sessions in three monkeys. Similar distributions were obtained for the individual monkeys, and the distributions were consistently more narrow during good epochs. (**C** to **F**) Poststimulus time histograms (PSTHs) for LC activity during the visual discrimination task. (C and D) Response for targets. (E and F) Response for distractors. (C and E) "Good" behavioral epochs. (D and F) "Poor" behavioral epochs (FA rate typically > 7%). Stimuli occur at time zero. All histograms are normalized to a standard of 100 trials. Similar results were obtained in another 29 single-cell recordings and 37 multicell recordings.

M. Usher, Department of Psychology, University of Kent, Canterbury, UK. J. D. Cohen, Department of Psychology, Princeton University, Princeton, NJ 08540, USA and Department of Psychiatry, University of Pittsburgh, Pittsburgh, PA 15213, USA. D. Servan-Schreiber, Department of Psychiatry, University of Pittsburgh, Pittsburgh, PA 15213, USA. J. Rajkowski and G. Aston-Jones, Department of Psychiatry, University of Pennsylvania, VAMC (151), University and Woodland Avenues, Philadelphia, PA 19104, USA.

*To whom correspondence should be addressed. E-mail: gaj@mail.med.upenn.edu

level of the phenomena it addresses.

The LC network is a population of 250 spiking neurons, each of which is a leaky integrate-and-fire cell (*6*, *7*) that exhibits temporal dynamics similar to those in compartmental models (*8*). In the model, LC cells interact with each other in two ways. First, lateral inhibition simulates the effect of local NE release (*9*, *10*). Second, a voltage-dependent interaction among LC units simulates the effects of hypothesized electrotonic coupling among LC neurons (*11*). In addition, each LC cell receives input from the behavioral network (see below), as well as noise that is responsible for a spontaneous firing rate of about 1 spike/s [as observed in vivo (*2*)].

The behavioral component of the model is a simple connectionist network, consisting of two input units (one for target and one for distractor stimuli), two corresponding decision units, and one response unit (Fig. 2A). Connections between units in different processing layers are excitatory (reflecting information flow), connections within a layer are inhibitory (competition), and the activity of units is subject to small random variations (noise) (*12*). Each input unit has a strong weight to the corresponding decision unit and a weaker projection to the other decision unit. The target decision unit has a positively weighted connection to the response unit and to the LC network (*13*). Finally, consistent with previous simulation work, we assume that NE release has the effect of increasing the gain of the activation function for units in the decision and response layers [see below and (*14*, *15*)].

A task trial was simulated by activating the input unit corresponding to the current stimulus, which resulted in the spread of activation to the competing units in the decision layer and then to the response unit and LC. Characteristic dynamic responses of different units in the behavioral network after presentation of each type of stimulus (in the absence of modulation by LC) are displayed in Fig. 2B.

The simulated pattern of LC firing with and without electrotonic coupling, after target and distractor stimuli, is shown in Fig. 3. Target stimuli evoke a transient, synchronized LC response as a result of input from the target decision unit to LC cells. The target-evoked response is terminated by NE-mediated collateral inhibition within the LC. Electrotonic coupling among LC neurons has two main effects. First, coupling causes a stronger response of the LC population to target inputs, as a result of the reinforcement of spike-induced depolarizations in each individual neuron by similar, simultaneous depolarizations in other LC cells within the population. Second, coupling reduces the spontaneous (tonic) firing rate of LC cells by mutually shunting the effect of uncorrelated noise on each cell's membrane potential (*16*). These simulation results closely resemble the patterns of monkey LC discharge observed during epochs of intermediate (versus high) tonic activity and good (versus poor) behavioral performance (Figs. 1 and 3).

As noted above, the output of the target decision unit provides input to the LC net-

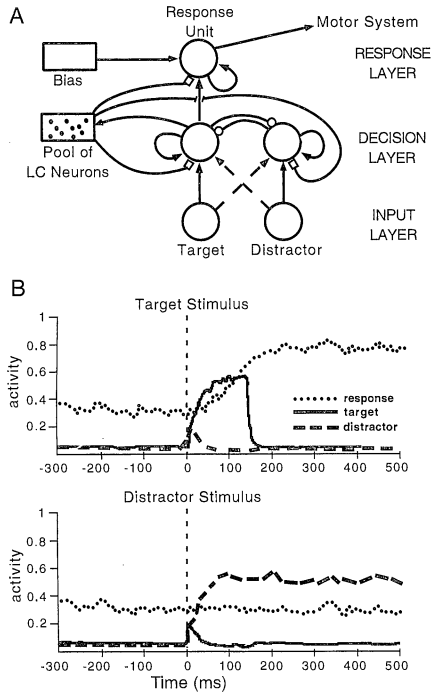

Fig. 2. (**A**) Architecture of the model of task performance. Arrows represent excitatory links and small circles represent inhibition. There is a moderate positive bias on the response unit, which captures the observation that monkeys in this task make many FAs but very few misses (*2*). (**B**) Dynamic trajectories of the target, distractor, and response assemblies (as indicated), in response to targets (top) or distractors (bottom). Stimulus presentation is at time zero. Solid lines, target unit; dashed lines, distractor unit; dotted lines, response unit. In response to each stimulus, there is partial activation of both target and distractor decision units due to their overlapping connections with the input. However, because of mutual competition, after about 100 ms, the decision unit corresponding to the activated stimulus typically prevails, and the competing unit is suppressed. When the target unit prevails, the activity of the response unit is driven above threshold, and a response is recorded. FAs occur because of noise in the response unit, which interacts with transient activation of the target decision unit by a distractor stimulus to produce a response. A threshold is set for activation of the response unit (0.6).

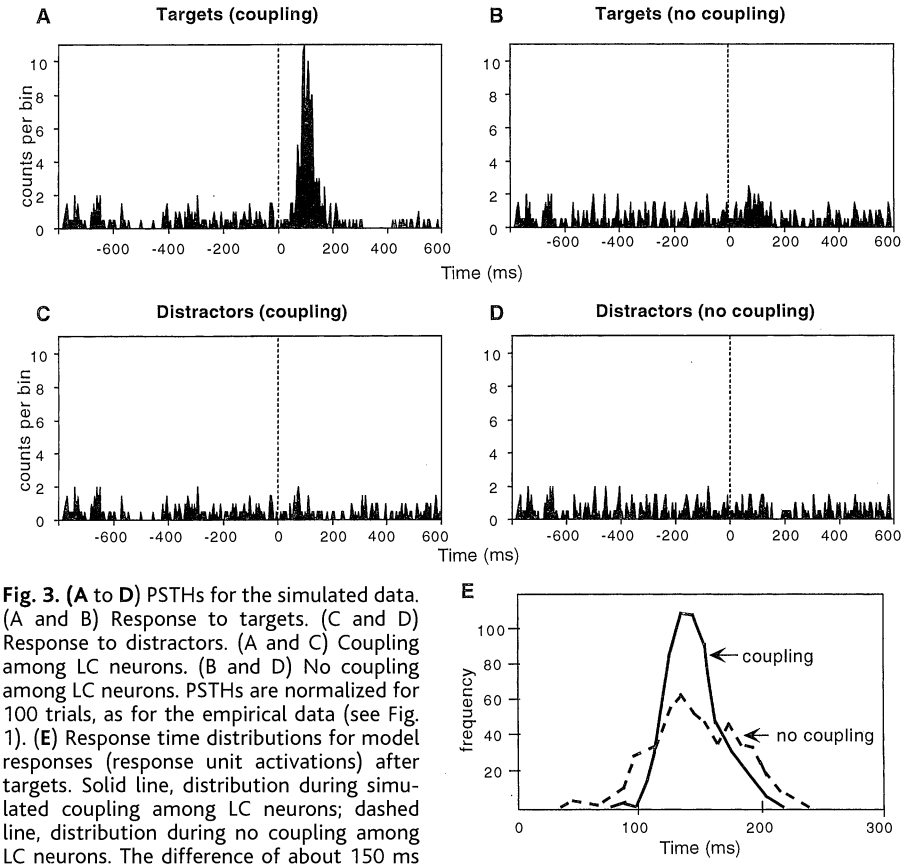

Fig. 3. (**A** to **D**) PSTHs for the simulated data. (A and B) Response to targets. (C and D) Response to distractors. (A and C) Coupling among LC neurons. (B and D) No coupling among LC neurons. PSTHs are normalized for 100 trials, as for the empirical data (see Fig. 1). (**E**) Response time distributions for model responses (response unit activations) after targets. Solid line, distribution during simulated coupling among LC neurons; dashed line, distribution during no coupling among LC neurons. The difference of about 150 ms between the latencies of empirical (Fig. 1B) and simulated behavioral responses (E) is consistent with a residual sensory or motor latency.

work, whereas LC activity modulates the gain of units in the decision and response layers of the behavioral network. Unlike in previous models, where the effect of catecholamines on cognitive performance was modeled as a fixed gain parameter throughout a simulation (*15*), here the value of the gain was determined dynamically by the output of the LC network. Thus, the synchronized, transient responses to target stimuli during epochs of high coupling (Figs. 1, C to F, and 3, A to D) resulted in a temporally modulated process. The effect of LC on the performance of the behavioral network can be seen by comparing the activation of the response unit under conditions of high and low coupling among LC neurons. Increased coupling among LC neurons produced a reduction in FAs (from 12 to 2%), without an increase in misses, and a significant narrowing of the RT distribution, without a change in the mean (Fig. 3E). Thus, a change in coupling among LC neurons in the model reproduces the changes in LC activity, behavioral performance, and the relation between these that is observed empirically.

Changes in electrotonic coupling produce the associated changes in behavior for several reasons. First, increased coupling reduces tonic LC activity, reducing NE release in the behavioral network and thereby lowering the responsivity of those units. For the response unit, this is equivalent to raising its threshold (*15*), which reduces the number of FAs and anticipatory responses. Ordinarily, raising the response threshold would also increase the number of misses and lengthen mean RT. However, increased coupling enhances evoked LC responses to target stimuli. The enhanced LC response produces a transient reduction in threshold specifically and shortly after target stimuli, which compensates for the overall increase in response threshold and potentiates the processing of target stimuli. This averts an increase in misses or RT (*17*). This temporal modulation of processing, with maximal gain occurring shortly after a target stimulus, is consistent with an attentional window reported in the cognitive literature (*18*) and also with recently proposed mechanisms for attentional modulation based on neural synchrony (*19*). Moreover, this mechanism has the combined effect of eliminating anticipations and of speeding up slow responses, explaining the observed narrowing of the RT distribution during the good behavioral epochs (Figs. 1B and 3E). Thus, a change in a single parameter (an increase in coupling within LC) can account for the reduction in tonic LC activity, the enhanced target-evoked phasic responses, and the association of this pattern of LC activity with a reduction of FAs and a tightening of the RT distribution in behavioral performance.

The model makes the prediction that improved performance is associated with increased electrotonic coupling and therefore should also be associated with greater synchrony in the spontaneous firing of LC neurons (Fig. 4B) (*20*). We tested this prediction by comparing cross correlograms generated for pairs of simultaneously recorded LC neurons during epochs of good and poor performance. Consistent with our prediction, we found that 18 of 23 pairs of recorded neurons exhibited a central peak in cross correlograms during epochs of good performance that was not present for the same neurons during poor performance (Fig. 4, A and B). Quantitative analyses of correlograms for these 23 pairs of cells indicated that the central peak during good performance was significantly greater than during poor performance.

Our simulation results suggest that electrotonic coupling may be an important mechanism underlying patterns of LC activity and may play a role in regulating behavioral performance. Strong evidence for coupling within the LC of neonatal rats has been reported (*21*). Although electrotonic coupling appears to decrease postnatally, recent studies indicate that coupling may persist in the LC of the adult rat (*22*, *23*). However, the presence of such coupling in the adult primate has not yet been empirically demonstrated. The model we have developed, together with the data regarding synchronization of LC activity, support this possibility and indicate that modulation of electrotonic coupling may produce potent effects on behavioral performance (*24*).

One important question concerns the adaptive advantage of the changes in behavior that are produced by changes in LC activity. In our model, intermediate tonic LC activity (due to increased coupling) facilitates a state of selective responding. This state is beneficial in a stable environment such as in our experimental task, where the source of reward is predictable and the behaviors relevant for acquiring it are known and consistent. However, what are the advantages of high tonic LC activity, which is associated with impaired performance in our experimental task? One possible answer is that heightened selectivity may at times be disadvantageous, such as in an uncertain or stressful environment, in which unexpected but imperative stimuli occur (for example, prey suddenly faced with a predator), or when previously reinforced responses lose their reward value (for example, satiety). Such circumstances require reevaluation of the sensory environment and abandonment of current behaviors in the search for more adaptive ones. This ability may also be critical for normal developmental and learning processes, as suggested by recent findings indicating that the best predictor of success in acquiring a new skill is not the speed with which the correct behavior is first discovered but the number of alternatives that are initially explored (*25*). According to our model, high tonic LC activity (as a result of low coupling) can provide a mechanism for sampling new stimuli and behaviors by reducing attentional selectivity and increasing behavioral responsiveness to unexpected or novel stimuli.

These considerations suggest that a tension exists between optimizing performance in a stable environment and favoring more flexible behavior in a changing or unfamiliar environment or when current rewards lose their value. This is a fundamental trade-off, which has been recognized in computational theories of reinforcement learning that distinguish between states that favor "exploitation"

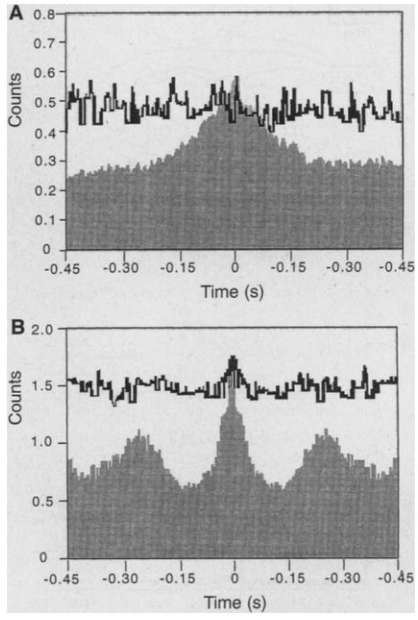

Fig. 4. Cross correlograms for two simultaneously recorded LC neurons during epochs of good (filled histograms) versus poor (contour lines) performance for the data (**A**) and for coupling versus no coupling, respectively, in the model (**B**). Note the central peak indicating synchronous activity during good performance (coupling), which is not present during poor performance (no coupling). Average amplitudes of central peaks in the data correlograms were compared as described in (*30*). Epochs analyzed were at least 500 s in duration. Epochs of target-evoked responses were eliminated by omitting 0.8 s of activity from each cell after target stimuli to avoid any bias produced by the synchrony of firing associated with phasic LC responses that occur primarily during epochs of good performance (coupling); this had no apparent effect on the cross correlograms obtained. Central peaks were significantly greater during good compared with poor epochs (8.08 ± 2.96 compared with 2.64 ± 1.08, respectively; $P < 0.05$; $n = 23$ pairs of neurons), whereas the spontaneous rate (baseline) was higher for the poor epochs. Similar results were obtained for pairs of neurons recorded from the same electrode and from two different electrodes.

of existing behavioral routines versus "exploration" of new ones (*26*). The mechanisms responsible for shifting between such states have not been specified. Our model indicates that changes in the mode of LC functioning (produced by alterations of electrotonic coupling) may provide a neural mechanism for mediating such shifts. This hypothesis also helps to integrate previously proposed roles for LC function (*27*). Future research is needed to directly test this hypothesis (*28*) and to characterize the neural system or systems providing input to the LC that are responsible for monitoring the current behavioral context and altering coupling among LC neurons when shifts of state are appropriate. It will also be important to determine the relation of the LC-NE neuromodulatory system to others, such as the dopamine system, that are thought to regulate behavior based on expectations about future events (*29*).

References and Notes

1. W. Schultz, P. Dayan, P. R. Montague, *Science* **275**, 1593 (1997).
2. G. Aston-Jones, J. Rajkowski, T. Alexinsky, *J. Neurosci.* **14**, 4467 (1994); J. Rajkowski, P. Kubiak, G. Aston-Jones, *Brain Res. Bull.* **35**, 607 (1994).
3. Training and experimental recording sessions took place in an acoustically insulated, electrically shielded metal chamber (IAC, Bronx, NY). Monkeys were trained to depress a lever and to stably foveate a fixation stimulus on a video monitor, at which point this stimulus was replaced by a target or nontarget stimulus (horizontally or vertically oriented rectangle). The animal was required to selectively release the lever in response to the target stimulus (20% of trials). Responses to the other stimulus were not reinforced but instead generated a 3-s time-out. Training continued until animals performed at a level of at least 85% correct. See (*2*) for more details.
4. Typically, epochs of poor performance contained more than seven times the frequency of FA errors as epochs of good performance. The hit rates varied only slightly between these periods, remaining either constant or declining slightly during poor performance intervals. For the three monkeys analyzed, the d' values in poor compared with good periods increased from 2.9 to 5.1, 3.7 to 4.7, and 3.7 to 5.1. The response criterion b also increased during the good periods from 0.23 to 0.82, 0.36 to 2.92, and 0.06 to 1.11, respectively. For these monkeys, the standard deviations of RTs were 58, 55, and 46 ms, respectively, during poor intervals and 35, 33, and 35 ms, respectively, during epochs of good performance ($P < 0.001$; Levene test of variances).
5. S. L. Foote, G. Aston-Jones, F. E. Bloom, *Proc. Natl. Acad. Sci. U.S.A.* **77**, 3033 (1980); S. J. Grant, G. Aston-Jones, D. E. J. Redmond, *Brain Res. Bull.* **21**, 401 (1988).
6. B. Knight, *J. Gen. Physiol.* **59**, 734 (1972).
7. Each LC cell integrates its input current (see below) and fires when its voltage at time t, $V(t)$, reaches threshold (V_{th}), after which it is artificially reset to rest ($V = 0$) and remains refractory until its voltage begins to rise again. We chose a refractory period of 10 ms, to mimic the afterhyperpolarization that follows individual LC spikes, $V_i(t + 1) = \lambda V_i(t) + I_i$, where λ is related to the membrane integration constant and I_i is an input current that depends additively on the activity of the target cell assembly x_1, the total amount of NE, and the hypothesized gap-junction current I_i^g (see below) and is also affected by uncorrelated Gaussian noise. The gap-junction current $I_i^g \propto \Sigma_j(V_j - V_i)$ on each LC unit is proportional to the sum of the ohmic currents contributed by the other LC units (which depend on the differences in voltage); for spiking neurons, V_j is taken as $V_{spike} = 5V_{th}$.
8. O. Bernander, C. Koch, M. Usher, *Neural Comput.* **6**, 622 (1994).
9. G. K. Aghajanian, J. M. Cedarbaum, R. Y. Wang, *Brain Res.* **136**, 570 (1977); T. M. Egan, G. Henderson, R. A. North, J. T. Williams, *J. Physiol.* **345**, 477 (1983); M. Ennis and G. Aston-Jones, *Brain Res.* **374**, 299 (1986).
10. Lateral inhibition occurs with a rise time of about 25 ms after LC cell firing and a decay of 250 ms [S. L. Foote, F. E. Bloom, G. Aston-Jones, *Physiol. Rev.* **63**, 844 (1983)]. This collateral NE release regulates the firing rate of the LC population: After each target-evoked, synchronized response of the population (see below), a slightly delayed inhibitory effect appears (as reflected in the PSTH histograms; Figs. 1C and 3A).
11. Electrotonic coupling is consistent with observations of gap junctions among LC neurons in neonatal rats (*21*) and with recent evidence for coupling among LC neurons in the adult rat (*22*, *23*). We assume that coupling produces a weak ohmic conductance between pairs of cells, which reaches a maximum of about 2.5% of the input current received by the cell, corresponding to the amount of current found in gap junctions identified in neonatal LC neurons (*21*).
12. This network is not intended to be a detailed simulation of specific neuronal circuits at the cellular level. Rather, it is intended to simulate task performance, with mechanisms that are consistent with those of biological information processing [see, for example, J. L. McClelland, in *Attention and Performance*, vol. XIV (MIT Press, Cambridge, MA, 1993), pp. 655–688; D. E. Rumelhart and J. L. McClelland, *Parallel Distributed Processing* (MIT Press, Cambridge MA, 1986)]. For example, the behavior of cell assemblies thought to represent task-relevant stimuli and responses in the cortex is simulated as single processing units with continuous-valued activation levels, on the assumption that information is represented in the cortex as the average spike rate of cell populations [D. J. Amit, *Modeling Brain Function* (Cambridge Univ. Press, Cambridge, 1989)]. Recurrent self-connections simulate mutual excitatory synapses between cells that belong to a particular assembly.
13. The weak weight from each input unit to the opposite decision unit captures our assumption that the stimuli used in the task have overlapping features and therefore each partially activates the representation of the other. The weights from the distractor decision unit to the response unit and LC network are zero (and therefore not implemented). This value corresponds to our assumption that, because the animal has been overtrained to respond to the target but not the distractor, there has been selective strengthening of projections from the target decision unit to the response unit and LC module, but not for the distractor unit.
14. The gain parameter g is an amplification factor that multiplies the net input to each unit, i, in its transfer activation function (a_i) (*15*): $a_i(t) = 1/\{1 + \exp[-g \times \text{netinput}_i(t)]\}$ and $\text{netinput}_i(t)$ is computed from the activations at the previous iteration step as

$$\text{netinput}_i(t) = \tau\left(\sum_j \text{activity}_j \times \text{weight}_{ij}\right) + (1 - \tau)[\text{netinput}_i(t - 1)]$$

for all units j that project to unit i with weight_{ij} and processing rate τ. The gain parameter is determined by the summed output of units in the LC network, with a lag time of about 55 to 90 ms between a change in mean LC unit activity and the consequent change in the gain parameter of units in the behavioral network (consistent with physiological data concerning the time constants governing LC activity and cortical release of NE) (*10*). Note that the effect of NE on the behavioral network (gain modulation) is different than its local effects within the LC (inhibitory), consistent with empirical data regarding its effects in each of these areas (*10*). The gain effect in the behavioral network is consistent with more detailed hypotheses about the effects of NE on cortical circuits [M. E. Hasselmo, *Behav. Brain Res.* **67**, 1 (1995)].
15. D. Servan-Schreiber, H. W. Printz, J. D. Cohen, *Science* **249**, 892 (1990).
16. Even the weak degree of coupling implemented (*11*) produces significant synchronization of the LC population, as predicted by theoretical models of coupled phase oscillators [Y. Kuramoto, *Chemical Oscillators, Waves and Turbulence* (Springer-Verlag, Berlin, 1984); A. Sherman and J. Rinzel, *Proc. Natl. Acad. Sci. U.S.A.* **89**, 2471 (1992); S. Strogatz and R. Mirollo, *J. Stat. Phys.* **63**, 613 (1991)], and decreases spontaneous firing rate. The relative decrease in the spontaneous rate of discharge observed in our simulations (from 0.90 to 0.67 Hz) is similar to that observed empirically in LC cells during good behavioral epochs (2.95 to 2.01 Hz). To assess the specificity of this effect, we explored other schemes for simulating variations in LC firing, none of which reproduced the patterns in the empirical data. For example, increasing lateral inhibition [for example, G. Harris, Z. Hausken, J. Williams, *Neuroscience* **50**, 253 (1992)] or decreasing noise among LC cells both reduced tonic discharge and increased synchronization of activity [C. van Vreeswijk, L. F. Abbott, B. G. Ermentrout, *J. Comput. Neurosci.* **1**, 303 (1994)] but did not produce the amplification of stimulus-evoked responses observed empirically during epochs of good behavioral performance (Fig. 1, C compared with D). Conversely, other schemes such as induction of a low-threshold calcium conductance [H. Jahnsen and R. Llinas, *J. Physiol.* **349**, 227 (1984)] (not reported to exist in LC neurons) or simultaneously increasing inhibitory and target-evoked excitatory inputs can produce the amplification effect but do not lead to the reduction of tonic activity or increased synchrony.
17. Note, however, that if it were to occur immediately, it would also potentiate processing in the distractor unit, which is transiently activated by the target stimulus (see Fig. 2B). This would lead to an increase in misses (through competition with the target unit) as well as an increase in FAs. However, the target-evoked LC response occurs about 100 ms after target presentation, which is after the time interval of transient activation of the distractor unit.
18. Studies with rapid serial visual presentation methods [E. Weichselgartner and G. Sperling, *Science* **238**, 778 (1987); A. Reeves and G. Sperling, *Psychol. Rev.* **93**, 180 (1986); J. E. Raymond, K. L. Shapiro, K. M. Arnell, *J. Exp. Psychol. Hum. Percept. Perform.* **21**, 653 (1992)] have demonstrated that targets are most efficiently accessed during an attentional window of about 180 ms [for review, see H. E. Egeth and S. Yantis, *Annu. Rev. Psychol.* **48**, 269 (1997)].
19. LC phasic responses to targets (which modulate the gain of decision and response units in the model) are characterized by a concentration of spikes 80 to 150 ms after stimulus presentation, which is compensated by postactivation inactivity, so that only the temporal alignment, but not the total number of spikes, differs after target stimuli. Such synchronous activity in one part of a system can enhance transmission into a subsequent processing stage [M. Abeles, *Isr. J. Med. Sci.* **18**, 83 (1982)], resulting in attentional modulation [E. Niebur and C. Koch, *J. Comput. Neurosci.* **1**, 141 (1994)]. Our results extend this computational principle from cortico-cortical interactions to interactions between subcortical structures and the cortex.
20. Previous experimental studies have linked electrotonic coupling with an increase in synchrony of firing [for example, R. Llinas, R. Baker, C. J. Sotelo, *J. Neurophysiol.* **37**, 560 (1974); C. P. Taylor and F. E. Dudek, *Science* **218**, 810 (1982); A. Draguhn, R. Traub, D. Schmitz, J. G. R. Jefferys, *Nature* **394**, 189 (1998)].
21. M. J. Christie, J. T. Williams, R. A. North, *J. Neurosci.* **9**, 3584 (1989); M. J. Christie and H. F. Jelinek, *Neuroscience* **56**, 129 (1993).
22. M. Ishimatsu and J. T. Williams, *J. Neurosci.* **16**, 5196 (1996); R. A. Travagli, M. Wessendorf, T. V. Dunwiddie, J. T. Williams, *Soc. Neurosci. Abstr.* **20**, 1734

(1994); R. A. Travagli, T. V. Dunwiddie, J. T. Williams, *J. Neurophysiol.* **74**, 519 (1994).
23. P. B. Osborne and J. T. Williams, *J. Neurophysiol.* **76**, 1559 (1996).
24. Previous electrophysiological studies reveal that the adenylyl cyclase stimulator forskolin increases coupling among adult LC neurons, suggesting that coupling among these cells may be modulated by a cyclic adenosine monophosphate (cAMP)–dependent mechanism in the rat (*23*). A cAMP mechanism has also been described for modulated coupling in other central neurons, and such coupling has been found to be modulated within a time frame of seconds, consistent with the data and model presented here [D. G. McMahon and D. R. Brown, *J. Neurophysiol.* **72**, 2257 (1994); D. G. McMahon and M. P. Mattson, *Brain Res.* **718**, 89 (1996)].
25. R. S. Siegler, *Cognit. Psychol.* **28**, 225 (1995).
26. L. P. Kaelbling, M. L. Littman, A. W. Moore, *J. Artif. Intel. Res.* **4**, 237 (1996).
27. Our model provides an explicit mechanism that can account for the involvement of the LC system in selective attention [for example, N. R. Selden, T. W. Robbins, B. J. Everitt, *J. Neurosci.* **10**, 531 (1990); N. R. Selden, B. J. Cole, B. J. Everitt, T. W. Robbins, *Behav. Brain Res.* **39**, 29 (1990)] and in exploratory behavior and responsiveness to novelty [for example, S. J. Sara, C. Dyon-Laurent, A. Herve, *Cognit. Brain Res.* **2**, 181(1995); S. O. Ogren, T. Archer, S. B. Ross, in *Catecholamines: Neuropharmacology and Central Nervous System Theoretical Aspects*, M. Sandler, Ed. (Liss, New York, 1984), pp. 285–292)], by suggesting that each of these is associated with a different mode of LC function and that the LC may mediate shifts between them.
28. We have found in preliminary studies that direct manipulation of LC activity by local microinjections produces effects in task performance predicted by our model [S. Ivanova, J. Rajkowski, V. Silakov, T. Watanabe, G. Aston-Jones, *Soc. Neurosci. Abstr.* **23**, 1587 (1997)].
29. P. R. Montague, P Dayan, T. J. Sejnowski, *J. Neurosci.* **16**, 1936 (1996).
30. I. Nelken and E. A. Vaadia, *Biol. Cybern.* **64**, 51 (1990).
31. We thank M. Stemmler, E. Niebur, B. Waterhouse, and R. Zemmel for comments on the manuscript and S. Aston-Jones for illustrations. Supported by the Human Frontiers Science Program, Air Force Office of Scientific Research grant F49620- 93-1-0099, and National Institute of Mental Health grants MH47566, MH45156, MH 55309, and MH 58480.

17 August 1998; accepted 17 December 1998

Light-Gap Disturbances, Recruitment Limitation, and Tree Diversity in a Neotropical Forest

S. P. Hubbell,* R. B. Foster, S. T. O'Brien,† K. E. Harms, R. Condit, B. Wechsler, S. J. Wright, S. Loo de Lao

Light gap disturbances have been postulated to play a major role in maintaining tree diversity in species-rich tropical forests. This hypothesis was tested in more than 1200 gaps in a tropical forest in Panama over a 13-year period. Gaps increased seedling establishment and sapling densities, but this effect was nonspecific and broad-spectrum, and species richness per stem was identical in gaps and in nongap control sites. Spatial and temporal variation in the gap disturbance regime did not explain variation in species richness. The species composition of gaps was unpredictable even for pioneer tree species. Strong recruitment limitation appears to decouple the gap disturbance regime from control of tree diversity in this tropical forest.

When a tree dies in a closed-canopy forest, it creates a "light gap," a local disturbance that sets in motion a mini-successional sequence called gap-phase regeneration, which culminates in the replacement of the original canopy tree by one or more new trees (*1*). A widely accepted generalization in community ecology is that localized disturbances, such as treefall gaps, promote the coexistence of species having different resource use strategies and dispersal and competitive abilities—a hypothesis known as the intermediate disturbance hypothesis (*2*). A well-documented physiological and life-history trade-off exists in pioneers versus shade-tolerant mature forest trees in their degree of dependence on light and light gaps for germination, growth, and survival (*3*). At issue here is not whether such life history trade-offs exist or whether pioneers have an absolute requirement for gaps. The question is whether spatial and temporal variation in the gap disturbance regime is actually predictive of stand-to-stand variation in tree species richness and composition in particular tropical forests. If not, then the role of light gap disturbances in maintaining local tree diversity may need to be re-evaluated.

We tested the intermediate disturbance hypothesis in a 50-ha plot of old-growth tropical moist forest on Barro Colorado Island (BCI), Panama (*4*). All woody plants (excluding lianas) with a stem diameter of ≥1 cm dbh (diameter at breast height) have been tagged, measured, mapped, and identified to the species level (>300,000 stems comprising 314 species). Complete censuses have been conducted in 1982, 1985, 1990, and 1995 (*5*). From 1983 to 1996, we measured canopy height and gaps annually on a complete 5-m grid of 20,301 sample points (*1, 6*). From these data and the distribution of each species, we classified species into three regeneration niche guilds: strongly gap-dependent pioneer species, shade-tolerant species, and intermediate species (*7*). Through 1995, we monitored changes in 1985 sapling communities (stems 1 to 3.9 cm dbh) in all 1983 gap sites (canopy height <5 m) and nongap control areas. Control areas comprised the 28.1% of the 50-ha plot that remained in undisturbed high canopy (≥20 m) mature forest for the entire 13-year period. Because stem density increases in gap areas, we normalized species richness by dividing by number of stems. We compared species richness per stem in all 20 m by 20 m quadrats containing a gap in 1983 with nonoverlapping quadrats from control areas. We also tested for a relationship between the frequency of canopy disturbance and the 1995 species richness in the sapling community (*8*). Using a gap-focused method, we tested for an effect of gap size on species richness (*9*). In 1985, 1990, and 1995, we analyzed the sapling communities in same-aged (2-year-old) gaps created in 1983, 1988, and 1993. We analyzed the species richness and composition of sapling assemblages as a function of gap size for the three regeneration niche guilds. The disturbance regime in the BCI forest produces frequent but small light gaps from the death of one to several canopy trees (Fig. 1A). There are no records of severe disturbances such as hurricanes ever striking central Panama or BCI. Gaps varied over a 46-fold size range from 25 m^2 to the largest gap of 1150 m^2. Light gaps markedly increased sapling stem densities relative to nongap, mature forest control sites ($P < 0.001$). Gaps of 25 m^2 were legitimately included in the analysis, because pioneer species successfully germinated, survived, and grew in them (Table 1).

As predicted by the intermediate disturbance hypothesis, quadrats containing light gaps had substantially more species than did quadrats in nongap, mature forest sites ($P <$ 0.001, Komolgorov-Smirnov test) (Fig. 2A).

S. P. Hubbell, S. T. O'Brien, B. Wechsler, Department of Ecology and Evolutionary Biology, Princeton University, Princeton, NJ 08544, USA. R. B. Foster, K. E. Harms, R. Condit, S. J. Wright, S. Loo de Lao, Smithsonian Tropical Research Institute, Post Office Box 2072, Balboa, Republic of Panama.

*To whom correspondence should be addressed. E-mail: shubbell@princeton.edu

†Present address: W. Alton Jones Foundation, 232 East High Street, Charlottesville, VA 22902, USA.